The Journal of Chemical Physics

Coarse grained open system quantum dynamics

Cite as: J. Chem. Phys. **129**, 194104 (2008); https://doi.org/10.1063/1.3010370
Submitted: 04 September 2008 • Accepted: 10 October 2008 • Published Online: 17 November 2008

Ioannis Thanopulos, Paul Brumer and Moshe Shapiro

View Online Export Citation

ARTICLES YOU MAY BE INTERESTED IN

Self-consistent hybrid approach for complex systems: Application to the spin-boson model with Debye spectral density
The Journal of Chemical Physics **115**, 2991 (2001); https://doi.org/10.1063/1.1385562

Non-Markovian evolution of the density operator in the presence of strong laser fields
The Journal of Chemical Physics **111**, 3365 (1999); https://doi.org/10.1063/1.479669

Numerically "exact" approach to open quantum dynamics: The hierarchical equations of motion (HEOM)
The Journal of Chemical Physics **153**, 020901 (2020); https://doi.org/10.1063/5.0011599

Challenge us.
What are your needs for periodic signal detection?
Watch

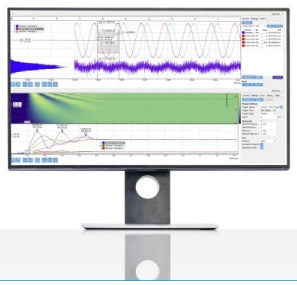

Zurich Instruments

© 2008 American Institute of Physics.

AIP Publishing

Coarse grained open system quantum dynamics

Ioannis Thanopulos,[1,a] Paul Brumer,[2] and Moshe Shapiro[1,3]
[1]*Department of Chemistry, The University of British Columbia, Vancouver V6T 1Z3, Canada*
[2]*Chemical Physics Theory Group, Department of Chemistry, and Center of Quantum Information and Quantum Control, University of Toronto, Toronto, Ontario M5S 3H6, Canada*
[3]*Department of Chemical Physics, The Weizmann Institute, Rehovot 76100, Israel*

(Received 4 September 2008; accepted 10 October 2008; published online 17 November 2008)

We show that the quantum dynamics of a system comprised of a subspace $\mathcal{Q}$ coupled to a larger subspace $\mathcal{P}$ can be recast as a reduced set of "coarse grained" ordinary differential equations with constant coefficients. These equations can be solved by a single diagonalization of a general complex matrix. The method makes no assumptions about the strength of the couplings between the $\mathcal{Q}$ and the $\mathcal{P}$ subspaces, nor is there any limitation on the initial population in $\mathcal{P}$. The utility of the method is demonstrated via computations in three following areas: molecular compounds, photonic materials, and condensed phases. © *2008 American Institute of Physics*. [DOI: 10.1063/1.3010370]

I. INTRODUCTION

Simulating the dynamics of open quantum systems is one of the most important and challenging problems in physics and chemistry.[1–3] The objective here is to develop an efficient method for computing the quantum dynamics of a set of relatively small number of "interesting" states, belonging to subspace $\mathcal{Q}$, that are coupled to a much larger set of "less interesting" states, belonging to a (prediagonalized) subspace $\mathcal{P}$. Such an approach is necessary because a full dimensionality treatment incorporating all states in $\mathcal{Q}\cup\mathcal{P}$ is in general not feasible due to the formidable size of $\mathcal{P}$.

In the past, the effect of the subspace $\mathcal{P}$ on $\mathcal{Q}$ was introduced in limited following ways: by considering only short time dynamics, by considering only a particular range of $\mathcal{Q}$ and $\mathcal{P}$ coupling strengths, or by restricting the choice of initial populations of $\mathcal{Q}$ and/or $\mathcal{P}$.[1–3] Though it is possible to formulate the problem in general as a set of integrodifferential equations, these equations suffer from poor numerical stability, with their numerical solution usually demanding vast computational resources.

The recent introduction of time-independent partitioning techniques[4] for solving the system-bath problem has motivated us to look at the problem from the time-dependent point of view, enabling the inclusion of time-dependent system-bath couplings such as those introduced by laser fields. As described below, our approach invokes no particular assumptions and requires a single diagonalization of a general complex matrix. The result is a far more stable procedure than integrating a set of integrodifferential equations. Although the dimension of the matrix to be diagonalized is $q(M+1)$, where q is the dimension of $\mathcal{Q}$, and $M\approx 10-100$, may often be quite large, the method lends itself to various approximations that reduce the dimensionality but that still give accurate results for the time scales of physical interest.

This paper is organized as follows. We develop our methodology in Sec. II. Applications of our approach in the areas of molecular compounds, photonic materials and condensed-phases are discussed in Sec. III. We conclude in Sec. IV.

II. THEORY

We start the formal development by considering the Hamiltonian on the entire Hilbert space $\mathcal{H}$ given as $H=H(q_1,q_2,\ldots,q_N)$, where $\{q_1,\ldots,q_N\}$ describe the corresponding N degrees of freedom (DOF) of H. We are primarily interested in the set of states related to the $\{q_1,\ldots q_q\}$ set of DOF. The Hamiltonian on $\mathcal{H}$ is now written as $H(q_1,\ldots,q_N)=H_Q(q_1,\ldots,q_q,0,\ldots,0)+H_P(0,\ldots,0,q_{q+1},\ldots,q_N)+V^{QP}(q_1,\ldots,q_N)$, where we denote as H_Q and H_P the Hamiltonian defining the $\mathcal{Q}$ and $\mathcal{P}$ subspaces, respectively, and $V^{QP}\equiv H-H_Q-H_P$ denotes the interaction term between these subspaces. We note that the above procedure is applicable equally well to closed systems and system-plus-reservoir models, which traditionally are used for the study of open quantum systems,[2,3] where the Hamiltonian of the system-plus-reservoir is given in a microscopic form as function of its DOF, e.g., a multilevel system coupled to a reservoir described by (an)harmonic oscillators.[2,3]

Neither the states in $\mathcal{Q}$ nor the states in $\mathcal{P}$ are eigenstates of H. Rather, the states in $\mathcal{Q}$ obey the equation $(\mathcal{E}_\ell-H_Q)|\ell\rangle=0$ $(\ell=1,..,q)$, and the states in $\mathcal{P}$ obey the equation $(E^--H_P)|E,n^-\rangle=0$, where $|E,n^-\rangle$ form a continuum or a quasicontinuum of eigenenergies. Here n denotes all quantum numbers other than the energy E, and $E^-\equiv E-i\epsilon$. We use boundary conditions for the scattering solutions that correlate with a single freely moving state in the $\mathcal{P}$ space when the scattering process is over. We also use here, and throughout the paper, atomic units, for which $\hbar=1$.

It is possible to solve the dynamics in the entire $\mathcal{H}$ space by expanding Ψ, the solution of the time-dependent Schrödinger equation, $i\dot{\Psi}=H\Psi$, as

[a]Present address: Theoretical and Physical Chemistry Institute, National Hellenic Research Foundation, Athens 11635, Greece. Electronic mail: ithano@eie.gr.

 © 2008 American Institute of Physics

$$|\Psi(t)\rangle = \sum_{\ell=1}^{q} b_\ell(t) e^{-i\mathcal{E}_\ell t}|\ell\rangle + \int dE b_{E,n}(t) e^{-iEt}|E,n^-\rangle. \quad (1)$$

Substituting Eq. (1) into the time-dependent Schrödinger equation gives a set of ordinary differential equations,

$$\dot{b}_\ell(t) = i\int dE b_{E,n}(t)\mathcal{V}(\ell|E,n)e^{-i(E-\mathcal{E}_\ell)t}, \quad \ell = 1,\ldots,q, \quad (2)$$

$$\dot{b}_{E,n}(t) = i\sum_{k=1}^{q} b_k(t)\mathcal{V}^*(k|E,n)e^{i(E-\mathcal{E}_k)t}, \quad \text{for every } E, \quad (3)$$

with $\mathcal{V}(k|E,n) \equiv \langle E_k|V^{QP}|E,n^-\rangle$. These equations cannot be readily solved because of the huge number (which is in fact innumerable in the continuum case) of bath coefficients appearing in Eq. (3). We can however formally eliminate Eq. (3) by integrating them over time and substituting the resulting expressions into Eq. (2) to obtain

$$\dot{b}_\ell(t) = i\int dE b_{E,n}(0)\mathcal{V}(\ell|E,n)e^{-i(E-\mathcal{E}_\ell)t} + \sum_{k=1}^{q} e^{-i(\mathcal{E}_k-\mathcal{E}_\ell)t}\int_0^t dt' b_k(t')F_{\ell,k}(t-t'), \quad (4)$$

where

$$F_{\ell,k}(\tau) \equiv ie^{i\mathcal{E}_k\tau}\int dE\mathcal{G}_{\ell,k}(E)e^{-iE\tau}, \quad (5)$$

with $\tau \equiv t-t'$ and $\mathcal{G}_{\ell,k}(E)$, the spectral density in $\mathcal{P}$, being given as

$$\mathcal{G}_{\ell,k}(E) = \sum_n \mathcal{V}(\ell|E,n)\mathcal{V}^*(k|E,n). \quad (6)$$

The spectral density can be represented to the desired accuracy as a sum of *resonances*[5–8]

$$\mathcal{G}_{\ell,k}(E) = \frac{2}{\pi}\sum_{\lambda=1}^{M} W_\lambda^{\ell,k}\frac{G_\lambda}{4(E-\Omega_\lambda)^2+G_\lambda^2}, \quad (7)$$

with complex $W_\lambda^{\ell,k}$ and real Ω_λ and G_λ.

The above expansion which can always be performed (although often some of the resonances may be broad and overlap one another) recasts $F_{\ell,k}(\tau)$, the correlation functions of Eq. (5), as a sum of exponentials,

$$F_{\ell,k}(\tau) = i\exp(i\mathcal{E}_k\tau)\sum_{\lambda=1}^{M} W_\lambda^{\ell,k}e^{-i\Omega_\lambda\tau-G_\lambda|\tau|/2} \equiv i\exp(i\mathcal{E}_k\tau)\mathcal{F}_{\ell,k}(\tau). \quad (8)$$

As in most finite fitting procedures, the set of fitting parameters $\{W_\lambda^{\ell,k},\Omega_\lambda,G_\lambda\}$ is not unique. This, however, need not detract from the quality of representation of $F_{\ell,k}(\tau)$, the goodness of which can be monitored by comparing $F_{\ell,k}(\tau)$ obtained via Eq. (8) with the correlation functions obtained by directly integrating Eq. (5).

The expansion of $F_{\ell,k}(\tau)$ as a sum of exponentials allows one to transform the integrodifferential equations of Eq. (4) into a set of ordinary differential equations. We obtain that

$$\dot{b}_\ell(t) = iK_\ell^0(t) + i\sum_{\lambda=1}^{M}\exp[i(\mathcal{E}_\ell-\Omega_\lambda)t]\mathcal{J}_\lambda^\ell(t), \quad (9)$$

with

$$\mathcal{J}_\lambda^\ell(t) = i\sum_{k=1}^{q} W_\lambda^{\ell,k}\exp(-G_\lambda t/2) \times\int_0^t dt' b_k(t')\exp[-i(\mathcal{E}_k-\Omega_\lambda+iG_\lambda/2)t'], \quad (10)$$

and

$$K_\ell^0(t) = \exp(i\mathcal{E}_\ell t)\int dE b_{E,n}(0)\mathcal{V}(\ell|E,n)\exp(-iEt). \quad (11)$$

Rather than use Eq. (10) directly, we note that the $\mathcal{J}_\lambda^\ell(t)$ mode amplitudes satisfy a set of first order differential equations,

$$\dot{\mathcal{J}}_\lambda^\ell(t) = \frac{i}{2}G_\lambda\mathcal{J}_\lambda(t) + i\sum_{k=1}^{q} W_\lambda^{\ell,k}b_k(t)e^{-i(\mathcal{E}_k-\Omega_\lambda)t}. \quad (12)$$

We have thus transformed the q integrodifferential equations of Eq. (4) into a set of $q\times(M+1)$ ordinary differential equations given by Eqs. (9)–(12).

Denoting $\tilde{b}_k(t) \equiv \exp(-i\mathcal{E}_k t)b_k(t)$ and $\tilde{\mathcal{J}}_\lambda^\ell(t) \equiv \exp(-i\Omega_\lambda t)\times\mathcal{J}_\lambda^\ell(t)$, we obtain our working equations,

$$\dot{\mathbf{c}}(t) = i\mathcal{K}\cdot\mathbf{c}(t) + i\mathbf{K}^0(t), \quad (13)$$

where $\mathbf{c}(t) = (\tilde{b}_1,\ldots,\tilde{b}_q,\tilde{\mathcal{J}}_1^1,\ldots,\tilde{\mathcal{J}}_M^1,\ldots,\tilde{\mathcal{J}}_1^q,\ldots,\tilde{\mathcal{J}}_M^q)^{\mathbf{T}} \equiv (\tilde{b}_1,\ldots,\tilde{b}_N,\tilde{\mathcal{J}}^{(1)},\ldots,\tilde{\mathcal{J}}^{(qM)})^{\mathbf{T}}$, with all $\tilde{\mathcal{J}}^{(i)}(0)=0$, and $\mathbf{K}^0(t) = (K_1^0,\ldots,K_q^0,0,\ldots,0)^{\mathbf{T}}$. Here $^{\mathbf{T}}$ is the transpose operation and $\mathcal{K}$ is a time-independent complex matrix, with a characteristic block structure given by

$$\mathcal{K} = \begin{pmatrix} \mathcal{S} & \mathcal{Y} \\ \mathcal{Z} & \mathcal{R} \end{pmatrix}, \mathcal{Z} = \begin{pmatrix} \mathbf{W}^{(1)} \\ \ldots \\ \mathbf{W}^{(qM)} \end{pmatrix}, \mathcal{Y} = \begin{pmatrix} \Omega^{(1)} \\ \ldots \\ \Omega^{(q)} \end{pmatrix}. \quad (14)$$

In Eq. (14), $\mathcal{S}_{k,k'} = \delta_{k,k'}\mathcal{E}_k$ and $\mathcal{R}_{i,i'} = \delta_{i,i'}(\Omega_\lambda + iG_\lambda/2)$ for the diagonal blocks. The $\mathbf{W}^{(i)}$ arrays of matrix $\mathcal{Z}$ are defined as $\mathbf{W}^{(i)} = (W_\lambda^{\ell,1},\ldots,W_\lambda^{\ell,q})$, and the $\Omega^{(i)}$ arrays of matrix $\mathcal{Y}$ are defined as $[\Omega^{(i)}]_{k,j}=1$ for $k+(i-1)\times M \le j \le k+i\times M$ and $[\Omega^{(i)}]_{k,j}=0$ otherwise. Here $k,k'=1,..,q$, $j=1,..,q\times M$, and $i,i'=\lambda+(\ell-1)\times M$, with $\lambda=1,..,M$ forming the inner loop and $\ell=1,..,q$ the outer loop.

Given these definitions, we write the solution of Eq. (13) as

$$\mathbf{c}(t) = \sum_j^{M'}\mathbf{\Lambda}_j e^{i\lambda_j t}\left(c_j^0 - i\int_0^t dt'[\mathbf{L}^{-1}\cdot\mathbf{K}^0(t')]_j e^{-i\lambda_j t'}\right), \quad (15)$$

where $M' = q\times(M+1)$ is the number of λ_j eigenvalues and $\mathbf{\Lambda}_j$ eigenvectors of $\mathcal{K}$. The columns of the $\mathbf{L} \equiv [\mathbf{\Lambda}_1,\ldots,\mathbf{\Lambda}_{M'}]$ matrix are the eigenvectors of $\mathcal{K}$, and $[\mathbf{L}^{-1}\cdot\mathbf{K}^0(t)]_j$ are the jth column vector of the $\mathbf{L}^{-1}\cdot\mathbf{K}^0(t)$ matrix. The vector of complex coefficients c_j^0 is given as $\mathbf{c}^0 = \mathbf{L}^{-1}\cdot\mathbf{c}(0)$. We note that since $\mathcal{K}$ is not Hermitian, $\mathbf{L}^{-1} \neq \mathbf{L}^\dagger$.

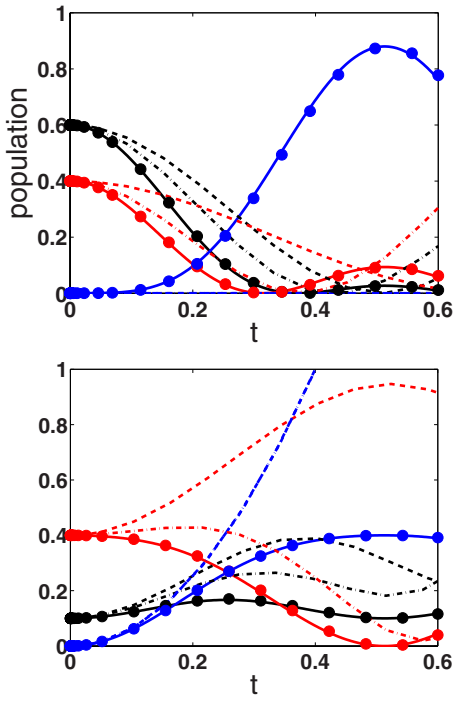

FIG. 1. (Color online) Coarse-grained population evolution of $|1\rangle$ (black lines), $|2\rangle$ (red lines), and $|3\rangle$ (blue lines) $\in \mathcal{Q}$ interacting with $p=50$ states $\in \mathcal{P}$, when $\mathcal{P}$ is initially empty (left panel) and half-populated (right panel). Results for $M=10$ (dashed lines), $M=30$ (dash-dotted lines), and $M=50$ (solid lines) are shown. The solution of the corresponding Schrödinger equation is also presented (solid circles). The $M=10$ (dashed) and $M=30$ (dash-dotted) state $|3\rangle$ curves (blue) coincide in both panels.

In the quasicontinuum case, the spectrum of H_P is made up of p discrete eigenvalues $(\mathcal{E}_\beta - H_P)|\beta\rangle = 0$. In that case, we equate the states $|E, n^-\rangle$ with vanishingly narrow resonances, and take Ω_λ of Eq. (7) to be the average of a (small) group of $\mathcal{E}_\beta$. When this is done, Eq. (15) describes a coarse grained dynamics in the $\mathcal{Q}$-space.

Below, we use two coarse-graining schemes, termed "coarse-grained $W_\lambda^{k,\ell}$" and "coarse-grained $V_{\lambda,\ell}$." The coarse-grained $W_\lambda^{k,\ell}$ scheme is obtained by first dividing the energy range of the $\mathcal{P}$ space into M bins with the bin centers corresponding to the energies of the largest $W_\lambda^{k,\ell}$. The coarse grained coefficients are then obtained by averaging over $W_\lambda^{k,\ell}$ within each bin. In the coarse-grained $V_{\lambda,\ell}$ scheme, we bin the energies according to the largest $V_{\lambda,\ell}$ values and average the $V_{\lambda,\ell}$ within each bin. Below we compare the coarse grained results with the "exact" numerical solution of the Schrödinger equation.

III. APPLICATIONS

In this section we present applications in various fields of the theory developed above. In Fig. 1, our method is applied to a toy model with $q=3$ states $\in \mathcal{Q}$ and $p=50$ states $\in \mathcal{P}$, when $\mathcal{P}$ is initially either empty (left panel) or half-empty (right panel). In this example, we use the coarse-grained $W_\lambda^{k,\ell}$ only. We further minimize the influence of this particular coarse-graining scheme by defining all energy levels $\in \mathcal{Q}$ and $\mathcal{P}$ to be degenerate, with zero energy, and all coupling matrix elements to be equal to 0.5. We note that our method which approximates the $\mathcal{P}$ space by introducing a small number of physically important effective modes, is probably less appropriate to such a model, where all modes are degenerate and equally strong, hence equally important. Nevertheless, we investigate this model because it constitutes a very stringent test of our methodology.

Computations based on choosing $b_E(0) \equiv \Sigma_\beta A_\beta(E)\mathcal{B}_\beta(0)$ in Eq. (11), with $\mathcal{B}_\beta(0)$ the initial coefficients of the $\mathcal{P}$ states, and $A_\beta(E) = \Gamma_\beta/(E - \mathcal{E}_\beta - i\Gamma_\beta/2)$, with ultimately vanishing Γ_β, are shown in Fig. 1. The reliability of the coarse-grained evolution of states $|1\rangle$ (black lines), $|2\rangle$ (red lines), and $|3\rangle$ (blue lines) is seen to depend primarily on the choice of M. Results are shown for $M=10$ (dashed lines), $M=30$ (dash-dotted lines), and $M=50$ (solid lines). For comparison, we also display in Fig. 1 (as solid circles) the exact numerical results obtained by solving the Schrödinger equation. The initial conditions in $\mathcal{Q}$ are $p_1=0.6$, $p_2=0.4$, and $p_3=0$ and $p_1=0.4$, $p_2=0.1$, and $p_3=0$, when $\mathcal{P}$ is initially empty and half-empty, respectively.

As $M \to p$, the coarse grained results of both panels (all colors) approach, as expected, the exact results. The convergence rate to the exact results is however different for different states and for different initial population in the $\mathcal{P}$-space. Thus, the evolution of state $|3\rangle$ shows agreement between the coarse-grained dynamics and the exact results over a shorter time span when the $\mathcal{Q}$-states are initially empty, as compared to the initially populated $\mathcal{Q}$-states case.

We now consider the use of this coarse-graining procedure for more realistic systems. We are especially concerned with systems characterized by a very large number of $\mathcal{P}$-states and a small number (often just one) of initially populated $\mathcal{Q}$-states. For such a case, we choose the vibrational dynamics of the H_2O molecule, whose internal space is described by three normal coordinates $\{Q_s^a, Q_s^s, Q_b\}$, corresponding to the H_2O antisymmetric stretch, symmetric stretch, and bending normal modes, respectively. The vibrational Hamiltonian is written as

$$H(Q_s^a, Q_s^s, Q_b) = H_{1d}(Q_s^a, 0, 0) + H_{2d}(0, Q_s^s, Q_b) + V_I(Q_s^a, Q_s^s, Q_b), \tag{16}$$

where $V_I \equiv V(Q_s^a, Q_s^s, Q_b) - V(0, Q_s^s, Q_b) - V(Q_s^a, 0, 0)$, with $V(Q_s^a, Q_s^s, Q_b)$ being the full (ground electronic-state) potential energy surface of H_2O.[9] We obtain the vibrational eigenstates as in Ref. 10 and define the $\mathcal{Q}$ space as $\mathcal{Q} = \{|v_s^a\rangle\langle 0|_P\}$, with $v_s^a = 0, .., 19$, with $|v_s^a\rangle$ denoting the eigenstates of H_{1d} and $|0\rangle_P$ denoting the lowest eigenstate of H_{2d}. The $\mathcal{P}$ space is defined as $\mathcal{P} = \{|\lambda\rangle_P |0_s^a\rangle\}$, with $\lambda = 1, .., p$ and $p = 10\,000$, where $|\lambda\rangle_P$ denote the eigenstates of H_{2d}.

Figure 2 shows the exact time evolution of the $|16\rangle|0\rangle_P$ $\mathcal{Q}$-state of energy 15 630 cm^{-1} (blue solid line in both panels) for initially unpopulated $\mathcal{P}$ space. Two coarse-grained dynamics are shown in panel (a) (green dashed line displaying the $M=50$ results and the red dot-dashed line representing the $M=100$ case). In panel (b), we display the results of solving the bound state analog of Eq. (3) whose size ($p=10\,000$) is reduced by performing $V_{\lambda,\ell}^{QP}$ coarse graining. As shown in Fig. 2(b), a much larger number ($M=1000$) of bins is needed to achieve comparable accuracy to the $W_\lambda^{k,\ell}$ coarse graining with $M=50-100$ bins. Both the $M=50$ and M

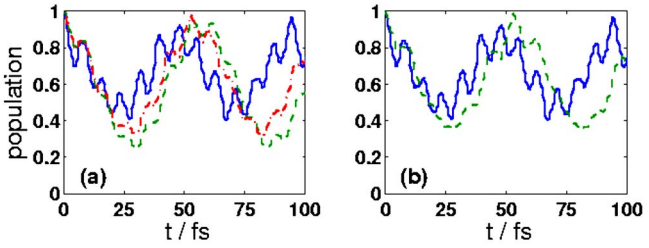

FIG. 2. (Color online) The dynamics of the $|16\rangle|0\rangle_P$ $\mathcal{Q}$-state when $\mathcal{P}$ is initially empty. Exact evolution (blue solid line, both panels), evolution of this state in the $W_\lambda^{k,\ell}$ coarse-graining procedure, with $M=50$ (green dashed line), and $M=100$ (red dot-dashed line) [panel (a)]. Panel (b): dynamics under the $V_{\lambda,\ell}$ coarse-graining procedure with $M=1000$ (green dashed line).

$=100$ coarse-grained dynamics displayed in panel (a) are in good agreement with the exact results for $t \leq 60$ fs. This time is larger than the $t_R \approx 50$ fs recurrence time for the state studied, as given by the exact results, beyond which the system dynamics is expected to be poorly approximated by the coarse-graining procedure used here, which is based on including in the dynamics the modes in $\mathcal{P}$ most strongly coupled to the $\mathcal{Q}$ space.

We next consider a continuous spectrum H_P where the spectral density is given *exactly* as a sum of resonances. We demonstrate that the simple formulas resulting from our methodology obviate the laborious numerical calculations used for such cases in the past. The case we have chosen is the Jaynes–Cummings Hamiltonian with detuning,[3] which describes non-Markovian spontaneous emissions to photonic band-gap materials.

When all the $\mathcal{P}$-modes are in the vacuum state, the spectral density is given as a single resonance term

$$\mathcal{G}(E) = w_0 G^2/[2\pi((E-\Delta-\omega_0)^2+G^2)]. \tag{17}$$

Figure 3 shows the dynamics of a single $\mathcal{Q}$-state coupled to the initially empty $\mathcal{P}$ space. The population $p_1(t)=|c_1(t)|^2 \in \mathcal{Q}$ is shown for the on-resonance case $\Delta=0$ (blue dashed line) and off-resonance $\Delta=8G$ case (red dot-dashed line),

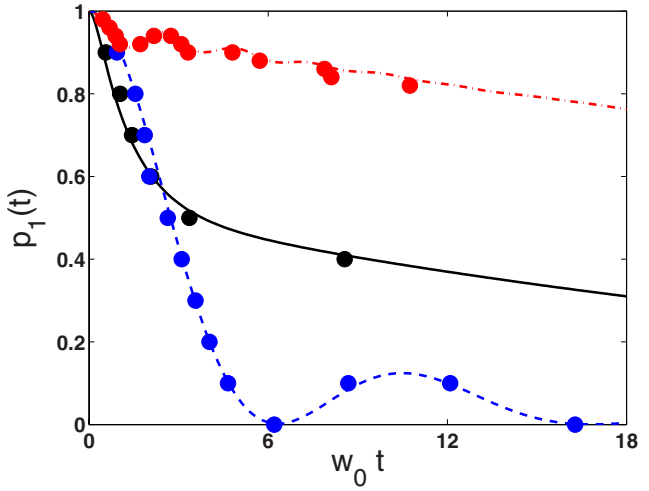

FIG. 3. (Color online) The Jaynes–Cummings model with detuning on resonance (blue dashed line) and off resonance (red dot-dashed line), as well as non-Markovian spontaneous decay into a photonic band gap (black solid line). The solid circles indicate corresponding results by previous works (Refs. 3 and 11).

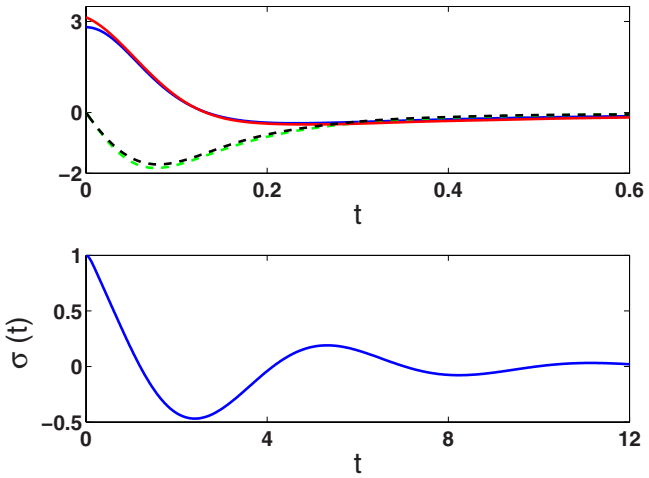

FIG. 4. (Color online) Top panel: Re$[C(t)]$ (blue solid line) and Im$[C(t)]$ (green dashed line) of the exact correlation function $C(t)$ for the Ohmic $\mathcal{G}^{\text{ohm}}(E)$ at zero temperature, and the real part (red) and imaginary part (black) of the correlation function obtained by fitting $\mathcal{G}^{\text{ohm}}(E)$ to Eq. (7) with $M=12$. Bottom: $\sigma(t) \equiv (|c_2(t)|^2 - |c_1(t)|^2)$ for two interacting states in $\mathcal{Q}$ coupled to an Ohmic, initially empty, $\mathcal{P}$ space, using the fitted spectral density with $M=12$.

under strong couplings, $G=0.2w_0$ and $G=0.3w_0$, respectively. In Fig. 3, we also present the population $p_1(t)$ (black solid line) of a single state in $\mathcal{Q}$ coupled to $\mathcal{P}$, with

$$\mathcal{G}(E) = \frac{\tilde{w}_0 w_1 G_1}{(E-\omega_0)^2 + G_1^2/4} - \frac{\tilde{w}_0 w_2 G_2}{(E-\omega_0)^2 + G_2^2/4}, \tag{18}$$

with $\tilde{w}_0 \equiv w_0^2/2\pi$, $w_1=1.1$, $w_2=0.1$, $G_1=10w_0$, and $G_2=w_0$, corresponding to non-Markovian spontaneous decay into a photonic band gap. All results in Fig. 3 are in excellent agreement with previous, purely numerical work[3] indicated by solid circles on the corresponding curves. We note that the purely numerical work involved intensive computational effort whereas the present method allows for almost a "back-of-the-envelope" calculation, involving the diagonalization of a small matrix.

We now consider a two state $\mathcal{Q}$ space, with $\mathcal{E}_1=\mathcal{E}_2=1$, interacting with an "Ohmic" $\mathcal{P}$ space, often used in condensed-phase studies, with $\mathcal{G}^{\text{ohm}}(E)=0.5\alpha E \exp(-E/E_c)$, where E_c is a cutoff energy and α is the coupling parameter. The corresponding correlation function $C(t)$, for initially empty $\mathcal{P}$, is analytically known[12] with

$$\text{Re}[C(t)] = \frac{\alpha E_c^2(1-E_c^2t^2)}{2(1+E_c^2t^2)^2}, \quad \text{Im}[C(t)] = \frac{\alpha E_c^3 t}{(1+E_c^2t^2)^2}.$$

We have used Eq. (7) with $M=12$ terms to fit the $\mathcal{G}^{\text{ohm}}(E)$ with $\alpha=0.1$ and $E_c=60$. The upper panel of Fig. 4 shows the Re$[C(t)]$ (blue solid line) and Im$[C(t)]$ (green dashed line) in comparison to Re$[\mathcal{F}(t)]$ (red dash-dotted line) and Im$[\mathcal{F}(t)]$ (cyan dotted line) of the correlation function $\mathcal{F}(t)$ using the fitted $\mathcal{G}(E)$. [We suppress the indices used in Eq. (7) since here $\mathcal{F}(t) \equiv \mathcal{F}_{1,2}(t)=\mathcal{F}_{1,1}(t)=\mathcal{F}_{2,2}(t)$.] Clearly, the agreement between $C(t)$ and $\mathcal{F}(t)$ is very good.

We consider the two states in $\mathcal{Q}$ being now coupled by $V_{1,2}^{\mathcal{Q}}=V_{2,1}^{\mathcal{Q}}=1$. These states are no longer eigenstates of H_Q. Nevertheless, our methodology is easily extendable to such cases by simply including the $V_{k,\ell}^{\mathcal{Q}}$ coupling elements in the $\mathcal{S}$

part of the $\mathcal{K}$ matrix of Eq. (14). In the lower panel of Fig. 4, we show $\sigma(t) \equiv (|c_2(t)|^2 - |c_1(t)|^2)$ for the states in $\mathcal{Q}$, assuming that the $\mathcal{P}$ space is in the vacuum state, using the fitted $\mathcal{G}(E)$ with $M=12$.

IV. CONCLUSION

We have developed a coarse-grained quantum dynamical approach that successfully treats the ubiquitous case of a small set of $\mathcal{Q}$-states coupled to a larger set of prediagonalized $\mathcal{P}$-states, with discrete or continuous spectrum. Cases where $\mathcal{P}$ is initially empty or initially populated have been examined in applications chosen from molecular physics, photonics, and condensed matter physics. Extensions to open system dynamics with an initially thermal bath can be easily made by applying this method to a sample of initial bath state and averaging over the results. Thus, the methodology presented here would provide a widely applicable approach for studying the dynamics of many open quantum systems.

ACKNOWLEDGMENTS

We gratefully acknowledge helpful discussions with E. Pollak, B. Garraway, E. Frishman, and E. A. Shapiro.

[1] Y.-J. Yan and R.-X. Xu, Annu. Rev. Phys. Chem. **56**, 187 (2005).
[2] U. Weiss, *Quantum Dissipative Systems* (World Scientific, Singapore, 1993).
[3] H.-P. Breuer and F. Petrucione, *The Theory of Open Quantum Systems* (Clarendon, Oxford, 2006).
[4] P. S. Christopher, M. Shapiro, and P. Brumer, J. Chem. Phys. **124**, 184107 (2006).
[5] E. Frishman and M. Shapiro, Phys. Rev. A **54**, 3310 (1996).
[6] C. Meier and D. J. Tannor, J. Chem. Phys. **111**, 3365 (1999).
[7] H. L. Friedman, F. O. Raineri, F. Hirata, and B.-C. Perng, J. Stat. Phys. **78**, 239 (1995); C. P. Koch, T. Klüner, H. J. Freund, and R. Kosloff, Phys. Rev. Lett. **90**, 117601 (2003).
[8] L. S. Cederbaum, E. Gindensperger, and I. Burghardt, Phys. Rev. Lett. **94**, 113003 (2005).
[9] D. F. Coker, R. E. Miller, and R. O. Watts, J. Chem. Phys. **82**, 3554 (1985).
[10] R. Marquardt, M. Quack, I. Thanopulos, and D. Luckhaus, J. Chem. Phys. **118**, 643 (2003).
[11] B. M. Garraway, Phys. Rev. A **55**, 2290 (1997); **55**, 4636 (1997).
[12] D. P. DiVincenzo and D. Loss, Phys. Rev. B **71**, 035318 (2005).